ARTICLES
PUBLISHED ONLINE: 30 NOVEMBER 2008 | DOI: 10.1038/NPHYS1151
nature physics

Superconducting nanocircuits for topologically protected qubits

Sergey Gladchenko[1], David Olaya[1], Eva Dupont-Ferrier[1], Benoit Douçot[2], Lev B. Ioffe[1] and Michael E. Gershenson[1]*

For successful realization of a quantum computer, its building blocks—the individual qubits—should be simultaneously scalable and sufficiently protected from environmental noise. Recently, a novel approach to the protection of superconducting qubits has been proposed. The idea is to prevent errors at the hardware level, by building a fault-free logical qubit from 'faulty' physical qubits with properly engineered interactions between them. The decoupling of such a topologically protected logical qubit from local noises is expected to grow exponentially with the number of physical qubits. Here, we report on proof-of-concept experiments with a prototype device that consists of twelve physical qubits made of nanoscale Josephson junctions. We observed that owing to properly tuned quantum fluctuations, this qubit is protected against magnetic flux variations well beyond linear order, in agreement with theoretical predictions. These results suggest that topologically protected superconducting qubits are feasible.

For implementation of quantum correction codes with realistic redundancy, the decoherence time of a qubit, τ_d, should be at least 10^4–10^5 times longer than the time of a single operation, τ_0 (refs 1,2). Unfortunately, all existing scalable qubits fall short of this criterion. For instance, at present, all superconducting qubits demonstrate error rates of $\varepsilon \sim 10^{-2}$ or larger[3–6]. The main reason for a relatively short decoherence time of superconducting qubits is their strong interaction with uncontrollable degrees of freedom in their environment, that is, 'noises' such as critical current fluctuations, charge noise, flux noise and quasiparticle poisoning[7,8]. Recent experimental and theoretical studies indicate that these noises are local, that is, they can be represented as a sum of operators acting on individual qubits. Because of the local nature of noises, the task of large-scale quantum computation is considered to be realistic[9,10]. Several approaches to the elimination of noise-induced decoherence have been proposed so far; these approaches are based on improving materials used for qubit fabrication[11,12] and decoupling of a qubit from local noises. In particular, the experiments[13–16] have shown that the qubit–noise coupling can be reduced by tuning the qubit control parameters. However, this tuning results only in a linear-order decoupling, which is insufficient for large-scale quantum computations.

Recently, an alternative approach to qubit protection has been proposed[17–20]. This approach is based on topological protection; it can be viewed as a hardware implementation of the software error correction protocols. The idea is to build a fault-free logical qubit from 'faulty' physical qubits with carefully tuned interaction between them. Such interactions result in a highly entangled collective state (similar to the one used in error correction schemes) protected by non-trivial symmetries from all local noises. The advantage of the topological protection is that it eliminates the need for high-fidelity ancilla-state preparation and measurements at the lowest level of error correction, thereby decreasing enormously the required redundancy. Here, we describe experiments with prototypes of topologically protected qubits that demonstrate the viability of this approach.

Design of the protected qubit

The prototype device studied here involves three levels of organization. Level 1 is constituted by the 'faulty' qubits shown as rhombi in Fig. 1. These Josephson elements with an effective energy

$$V_R = E_{2R}\cos(2\phi)$$

are implemented as superconducting loops interrupted by four Josephson junctions and threaded by the magnetic flux $\Phi_R = \Phi_0/2$ (refs 21–23). Here, $\phi = \pi\Phi_R/\Phi_0$ is the phase difference across each element; Φ_0 is the superconducting flux quantum. An individual Josephson junction is characterized by the Josephson energy $E_J = hI_c/2e$ and the charging energy $E_C = e^2/2C_J$; here, I_c and C_J are the critical current of the Josephson junction and its capacitance, respectively[24]. If E_C is negligible, each rhombus has two degenerate classical states separated by the energy barrier $2E_{2R} \approx 4(\sqrt{2}-1)E_J$ (see Fig. 1a). These states correspond to the phase difference $\phi = \pm\pi/2$ across the rhombus (the supercurrents circulate in a rhombus either clockwise or anticlockwise). A non-zero (but small) charging energy causes rare tunnelling events between these states and removes the degeneracy, resulting in the symmetric and antisymmetric superpositions: $|+\rangle_R = (1/\sqrt{2})(|\phi=-\pi/2\rangle + |\phi=\pi/2\rangle)$ and $|-\rangle_R = (1/\sqrt{2})(|\phi=-\pi/2\rangle - |\phi=\pi/2\rangle)$. These low-energy states of a rhombus are separated by a small energy gap $t \approx E_J^{3/4}E_C^{1/4}\exp(-1.6\sqrt{E_J/E_C})$. A single rhombus is not protected against local noises. Noise deforms the potential $V_R(\phi)$ and induces fluctuations of $2E_{1R}$, the energy difference between states $|\phi=\pi/2\rangle$ and $|\phi=-\pi/2\rangle$, which leads to dephasing. The deformed potential can be represented as $V_R(\phi) \approx E_{2R}\cos(2\phi) + E_{1R}\sin(\phi)$, where the second term describes both the effect of noise (the time-dependent part of E_{1R}) and an asymmetry of the rhombus (the time-independent part of E_{1R}).

To suppress dephasing, the 'cos(2ϕ)' Josephson elements are combined in a chain at level 2. The simplest two-element chain (Fig. 1b) connects a superconducting island to a current lead, the

[1]Department of Physics and Astronomy, Rutgers University, 136 Frelinghuysen Road, Piscataway, New Jersey 08854, USA, [2]Laboratoire de Physique Théorique et Hautes Energies, CNRS UMR 7589, Universités Paris 6 et 7, 4 place Jussieu, 75005 Paris, France. *e-mail: gersh@physics.rutgers.edu.

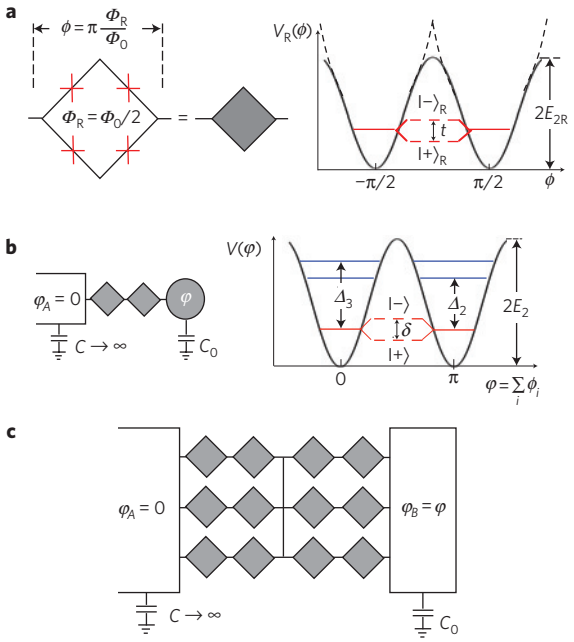

Figure 1 | Protected qubit based on '*cos*(2ϕ)' Josephson elements. **a**, The building blocks of the protected qubit are '*cos*(2ϕ)' Josephson elements (rhombi) implemented as superconducting loops interrupted by four Josephson junctions (red crosses) and threaded by the magnetic flux $\Phi_R = \Phi_0/2$. The Josephson energy of this 'faulty' physical qubit, $V_R = E_{2R}\cos 2\phi$, is doubly periodic in the phase difference ϕ across the rhombus. The black dashed lines show $V_R(\phi)$ in the classical limit ($E_C \to 0$); quantum fluctuations 'smear' the cusps at $\phi = n\pi$ and result in tunnelling between the states $|\phi = \pi/2\rangle$ and $|\phi = -\pi/2\rangle$. **b**, The simplest protected qubit is a chain of two cos(2ϕ) elements, which connects the rightmost 'island' to a large superconducting lead. Two degenerate classical states at $\varphi - \varphi_A = 0, \pi$ in the effective potential of the chain, $V(\varphi) = -E_2\cos 2\varphi$, are shown by solid red lines. A finite probability of tunnelling between the states $|\varphi = 0\rangle$ and $|\varphi = \pi\rangle$ removes the degeneracy and results in a small energy splitting δ between the logical states of the qubit, $(1/\sqrt{2})(|0\rangle \pm |\pi\rangle)$. The first and second excited levels are separated from this (almost) degenerate doublet by gaps Δ_2 and Δ_3, respectively. **c**, Connection of several rhombi chains in parallel increases the depth of the effective potential $V(\varphi)$ and suppresses the transitions between the qubit's logical states.

phase of which is fixed owing to a large capacitance C_0 (we choose $\varphi_A = 0$ in Fig. 1b). The logical variable is the superconducting phase difference across the chain, $\varphi - \varphi_A = \sum_i \phi_i$, which is the sum of the phase differences across individual rhombi. For an even number of rhombi in a chain, φ is either 0 or π. The double periodicity of the energies of rhombi leads to the double periodicity of the chain energy $V(\varphi) = -E_2\cos(2\varphi)$, where $E_2 = \hbar I_2/4e$ is determined by the critical current of the chain, I_2.

Quantum information is encoded in the (almost) degenerate ground states of the chain. For a two-rhombi chain, these states in the quasiclassical limit ($C_0 \to 0$) can be represented as

$$|\varphi = 0\rangle = \frac{1}{\sqrt{2}}\left(|\phi = -\pi/2\rangle\,|\phi = \pi/2\rangle + |\phi = \pi/2\rangle\,|\phi = -\pi/2\rangle\right),$$

$$|\varphi = \pi\rangle = \frac{1}{\sqrt{2}}\left(|\phi = -\pi/2\rangle\,|\phi = -\pi/2\rangle + |\phi = \pi/2\rangle\,|\phi = \pi/2\rangle\right).$$

The non-local logical states are protected from both relaxation and dephasing induced by local noises. The energy relaxation (transitions between states $|\varphi = 0\rangle$ and $|\varphi = \pi\rangle$) is suppressed because the energy barrier between the states, $2E_2$, prevents a single rhombus from flipping its phase by π. However, a pair of rhombi can flip simultaneously with the tunnelling amplitude t_{2R}. Remarkably, these flips induced by quantum fluctuations help suppress dephasing. Indeed, let us assume that the local noise changes the energy difference between states $|\phi = \pi/2\rangle$ and $|\phi = -\pi/2\rangle$ of the first and second rhombi by δE_1 and δE_2, respectively. Because the states of individual rhombi enter the logical states symmetrically, the noise does not affect the energy of these states in the first order of the perturbation theory. The difference in energies of the logical states appears only in the second order, $\delta E_{01} = (\delta E_1 \delta E_2/\Delta_2)$, where $\Delta_2 = 2t_{2R}$ is the gap that separates the logical states from the first excited state (see Fig. 1b). Thus, the chain is protected from dephasing provided Δ_2 is sufficiently large.

In a longer chain of N physical qubits, the effect of a local noise is expected to be suppressed up to the Nth order of the perturbation theory[18,20]. For example, the effective magnetic flux, which affects the logical states of the N-element chain, is greatly suppressed with respect to the flux noise $\delta\Phi_i = \Phi_i - \Phi_0/2$ (refs 18,20):

$$\delta\Phi_{\mathrm{eff}} = \prod_i^{N-1}\left(\frac{\delta\Phi_i}{\Phi_0}\frac{E_J}{\Delta_i}\right)\delta\Phi_i. \qquad (1)$$

Here, Δ_i is the excitation energy associated with changing the number of Cooper pairs by one on the superconducting 'island' shared by the ith and $(i+1)$th rhombi. The minimum value of $\Delta_i = \Delta_2$ corresponds to the excitation energy of the central island (this central island is shared among three chains in Fig. 1c). Note that $\delta\Phi_i = 0$ in a single rhombus results in $\delta\Phi_{\mathrm{eff}} = 0$ and, thus, the cos(2φ)-periodic energy of the whole chain. Equation (1) shows that for an efficient noise decoupling, the energy gap Δ_2 between the logical states and the first excited state of the qubit should be large (this is also required for decreasing the qubit operation time $\tau_0 > \hbar/\Delta_2$). The decoupling from other types of local noise is described by a similar formula with E_J being replaced by a relevant energy scale (for example, E_C for the charge noise). This decoupling is expected to be even more efficient because these energies are smaller than E_J.

The protection is maximized at level 3 by choosing an optimal interconnection between the elements and tuning the parameters of individual Josephson junctions. To realize large values of both E_2 and Δ_2, several conflicting requirements should be reconciled. Indeed, an increase of the number of rhombi in a chain improves the protection from noise. However, the energy barrier, which has to be high for protection, diminishes with N: $2E_2 \approx \pi^2 E_{2R}/2N$ in the quasiclassical limit ($C_0 \to \infty$) (ref. 25). This conflict can be resolved by parallel connection of several chains (see Fig. 1c). Similarly, quantum fluctuations help to establish a global coherent state across the chain, but, if excessively strong, they suppress the Josephson energy barrier between the logical states of a chain. Numerical simulations (see Supplementary Information) show that for each qubit architecture (M chains of N rhombi each), an optimal protection is realized for a certain value of the ratio E_J/E_C that controls the strength of quantum fluctuations. For example, for the tested design ($M = 3$, $N = 4$), sizable values of both E_2 and Δ_2 can be realized for $3 < E_J/E_C < 5$.

Protection testing: the idea of the experiment

The experiments described below were designed to test the key theoretical prediction (1), namely the decoupling from local noises well beyond the linear order. This test exploits the fact that equation (1) describes the decoupling of a qubit from both time-dependent flux noises and time-independent flux variations. This enabled us to experimentally test the protection in our arrays by studying their response to the static deviations of magnetic flux from its optimal value $\Phi_0/2$. For a single rhombus, the amplitude of the first harmonic, E_{1R}, in the expression for its potential

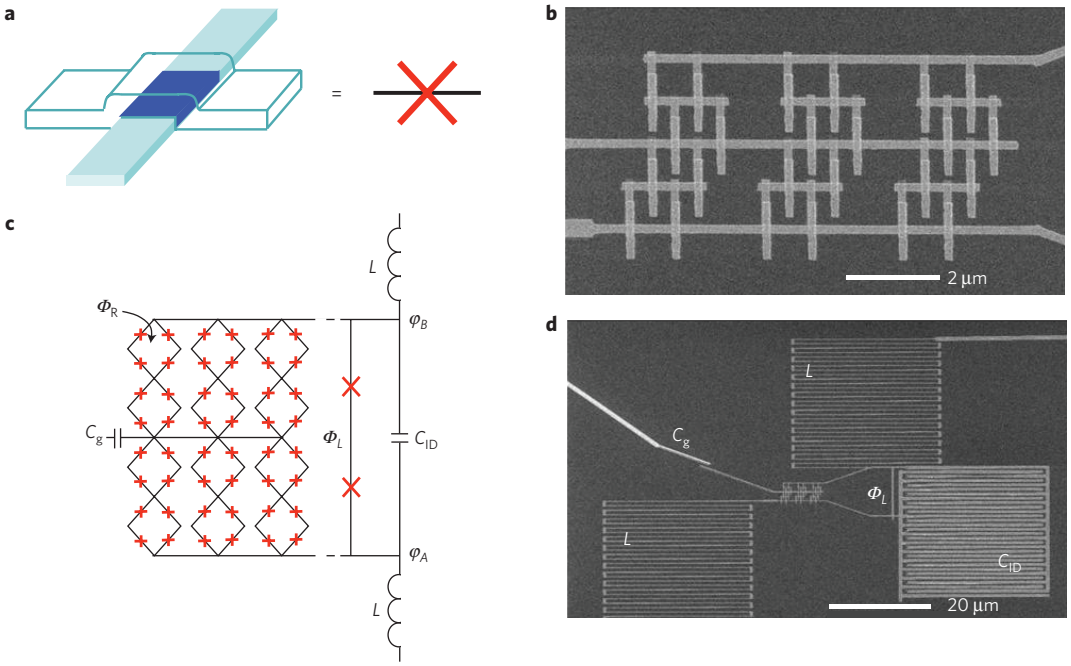

Figure 2 | The prototype of a protected superconducting qubit. a–d, Schematic design (**a**,**c**) and micrographs (**b**,**d**) of the device. Josephson junctions are formed at intersections of aluminium strips (the tunnel barrier is shown in blue in **a**). **b** shows micrographs of the array: three chains of rhombi connected in parallel to increase E_2. To probe $V(\varphi_{AB})$, the array is included in one 'arm' of a superconducting loop; another arm of the loop contains two larger Josephson junctions (**c** and **d**). The magnetic flux Φ_R through each rhombus of an area of 1 μm^2 controls the effective Josephson energy of the rhombi. The SQUID-like device is protected from external high-frequency noise and non-equilibrium quasiparticles generated outside the device by two meander-type inductances $L(\sim 2\times10^{-8}$ H). To ensure the 'classical' behaviour of larger Josephson junctions, the SQUID-like device is shunted by an inter-digitized capacitor $C_{ID} \sim 3\times10^{-14}$ F. The ends of the inductors are connected to the external circuit, which is used for the generation of current pulses.

Table 1 | Parameters of the studied devices.

Device	Area (μm^2)	R_N (kΩ)	E_C (K)	E_J/E_C
1	0.165 × 0.165	4.78	0.68	2.2
2	0.153 × 0.153	3.27	0.79	2.7
3	0.150 × 0.180	2.82	0.69	3.7
4	0.173 × 0.173	2.43	0.62	4.7
5	0.180 × 0.180	2.49	0.57	5.0

The values of R_N have been extracted from the total resistance of devices driven in the normal state by the current $I > I_{SW}$. The Josephson energy E_J for individual Josephson junctions has been determined from R_N using the Ambegaokar–Baratoff formula; the Coulomb energy E_C was estimated from the area of the junctions (C_J = (area) × 50 fF μm^{-2}; refs 24,31).

$V_R(\phi) \approx E_{2R}\cos(2\phi) + E_{1R}\sin(\phi)$ is proportional to $\delta\Phi = \Phi - \Phi_0/2$. Topological protection of a rhombi array would imply that the ratio E_1/E_2 in the expression for its energy, $V(\varphi) \approx -E_2\cos(2\varphi) - E_1\cos(\varphi)$, is exponentially reduced in comparison with that for a single rhombus: $E_1 \sim (\delta\Phi)^N$. The experiment was designed to measure the dependence $E_1(\delta\Phi)$ and to demonstrate that with proper tuning of quantum fluctuations, even a relatively small rhombi array is protected well beyond linear order.

The tested superconducting quantum interference device (SQUID)-like circuit (see Fig. 2) included the rhombi array and two larger (0.3 μm × 0.3 μm) Josephson junctions. The details of device design and fabrication are provided in the Methods section and Supplementary Information. We have tested several devices (see Table 1) with the normal-state resistance $R_N = 2.4$–5 kΩ and the ratio $E_J/E_C = 2$–5 for the individual Al–Al_2O_3–Al Josephson junctions in the rhombi. The phase difference φ_{AB} across the array was controlled by varying the magnetic flux Φ_L in the SQUID loop. Because of a large difference between the areas of individual rhombi (1 μm^2) and the SQUID loop (110 μm^2), the phase difference across the chains can be significantly varied without affecting the phase difference across individual rhombi.

Device response to static perturbations

The $V(\varphi_{AB})$ dependence of this underdamped Josephson device was studied by measuring the probability of switching of the device into the resistive state by 1-ms-long current pulses for different values of the external magnetic field B (for details, see Supplementary Information). Figure 3 shows the dependence of the switching current I_{SW} (defined as the pulse amplitude that switches the device into the resistive state with probability 0.5) on the magnetic field for a device with the ratio $E_J/E_C = 2.7$. The range of the magnetic field in Fig. 3a corresponds to the magnetic flux through a single rhombus, Φ_R, varying between $-\Phi_0/2$ and $\Phi_0/2$. The switching current oscillates with the magnetic flux Φ_L through the loop of the SQUID-type device with an area of ~110 μm^2. The period of oscillations, $\Delta\Phi_L$, depends on Φ_R : $\Delta\Phi_L = \Phi_0$ for all values of Φ_R except for $\Phi_R \approx (n + 1/2)\Phi_0$, where the period is halved ($\Delta\Phi_L = \Phi_0/2$). Note that in the quasiclassical case ($E_J/E_C > 20$),

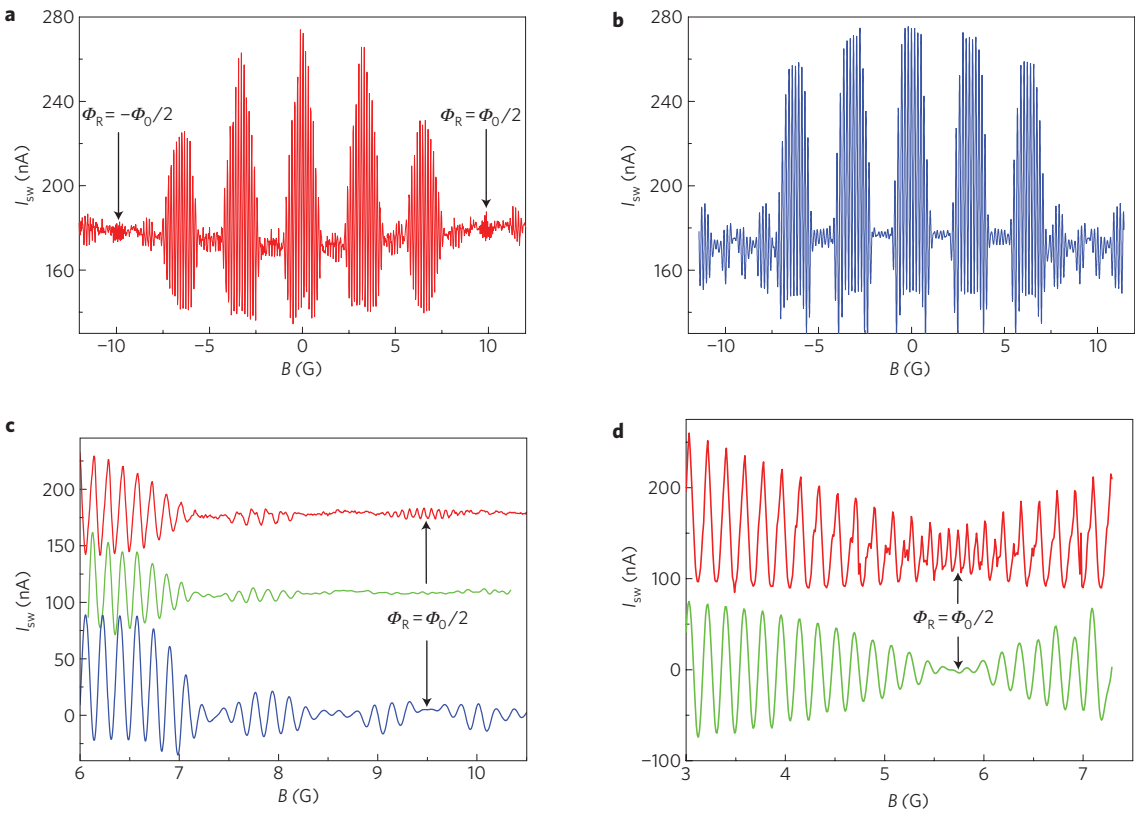

Figure 3 | Coherent transport of pairs of Cooper pairs. a, Oscillations of the switching current $I_{SW}(B)$, measured for device 2 at $T = 50$ mK, for the magnetic field corresponding to the flux through a single rhombus, Φ_R, ranging from $-\Phi_0/2$ to $\Phi_0/2$. **b**, Simulation of the first harmonic of I_{SW} oscillations (with a period of $\Delta\Phi_L = \Phi_0$). The calculations neglect quantum fluctuations and assume that the E_J values for individual Josephson junctions are randomly scattered within a ±20% interval. **c**, Comparison of the data and simulations in the protected regime ($\Phi_R \approx \Phi_0/2$). The red curve, which represents the experimental data, shows that I_{SW} oscillates with the period $\Delta\Phi_L = \Phi_0/2$ when $\Phi_R \approx \Phi_0/2$. The green curve (shifted down by 70 nA for clarity) shows the first harmonic of I_{SW} oscillations ($\Delta\Phi_L = \Phi_0$), which is strongly suppressed over a relatively wide range of magnetic fields around $\Phi_R = \Phi_0/2$. The calculated first harmonic is shown as the blue curve shifted down by 170 nA. **d**, The experimental data (red) and the first harmonic of oscillations (green, shifted down by 130 nA) for a single two-rhombi chain.

such a period halving has recently been observed[26]. The beatings of oscillations with $\Delta\Phi_L = \Phi_0$, observed at $\Phi_R/\Phi_0 \approx \pm 1/8$, $\pm 1/4$ and $\pm 3/8$, are due to the flux quantization in the intermediate-size loops between adjacent rhombi chains (the area of these loops is four times greater than the area of a single rhombus). Below, we focus on the regime $\Phi_R \approx (\pm 1/2)\Phi_0$, where the states $|\phi = \pi/2\rangle$ and $|\phi = -\pi/2\rangle$ of individual rhombi are almost degenerate and the rhombi array is expected to be protected from noise.

The oscillations of I_{SW} with the period $\Delta\Phi_L = \Phi_0$ vanish near $\Phi_R = \pm\Phi_0/2$ (Fig. 3c). In this regime, the effective Josephson energy of a rhombus, $V_R = E_{2R}\cos(2\phi)$, becomes small and the supercurrent of single Cooper pairs is blocked by quantum fluctuations. Comparison between the data obtained for the 4×3 rhombi array (Fig. 3c) and a single two-rhombi chain (Fig. 3d) shows that the oscillations with the period $\Delta\Phi_L = \Phi_0$ and, thus, the term $E_1\cos(\varphi)$ in the device energy, are suppressed for the array over a much wider range of magnetic fields. This observation is in good agreement with equation (1). Indeed, if the suppression is due to quantum fluctuation, the term $\cos(\varphi_{AB})$ responsible for the oscillations with the period $\Delta\Phi_L = \Phi_0$ should appear in the energy of a four-rhombi chain only in the fourth order in flux deviations from the optimal values $\Phi_R = (n+1/2)\Phi_0$. The direct computation of the effective Josephson coupling for the whole array in the fourth order in the perturbation theory gives

$$E_1 \approx \left(8.6\frac{\delta\Phi_R}{\Phi_0}E_J\right)^4 \frac{1}{\Delta_2\Delta_3^2}, \qquad (2)$$

where Δ_2 and Δ_3 are the energy gaps that separate two almost degenerate low-energy levels from the first and second excited levels, respectively (see Fig. 1b). Equation (2) translates into $E_1 \approx (40\delta\Phi_R/\Phi_0)^4 E_J$ for the array shown in Fig. 3c. Thus, the theory predicts that the term $\cos(\varphi_{AB})$ should be suppressed over the range $\delta\Phi_R = \pm 0.025\Phi_0$, in agreement with the experimental data. Observation of the $\cos(2\varphi_{AB})$ oscillations of I_{SW} together with the vanishing $\cos(\varphi_{AB})$ oscillations provides an essential test for the proper strength of quantum fluctuations. These experimental results also indicate that the scattering of Josephson junction parameters in the studied devices is relatively small: only the (axially) symmetric rhombi contribute to the order of protection, N.

The height of the energy barrier that separates the states of the rhombi array, $2E_2$, can be found from the amplitude $I_2 = 4eE_2/\hbar$ of the oscillations of switching current with period $\Delta\Phi_L = \Phi_0/2$. Figure 4 shows that the values of $2E_2/E_C$ measured for devices with different values of E_J/E_C are in good agreement with our numerical simulations (for simulation details, see Supplementary Information). The observed agreement verifies the validity of theoretical assumptions, which have also been used in the calculations of Δ_2 (see Fig. 4). The gap Δ_2 is the smallest of two gaps: the gap $2t_{2R} \sim t^2/E_J$ is associated with the excitations inside the chain with φ being fixed, whereas the other gap ($\sim\sqrt{32E_2E_C}$) is associated with the fluctuations of φ around its classical value. In the quasiclassical case ($E_J/E_C \gg 1$), Δ_2 coincides with $2t_{2R}$ (ref. 19). However, the realization of a sizable Δ_2 requires not-

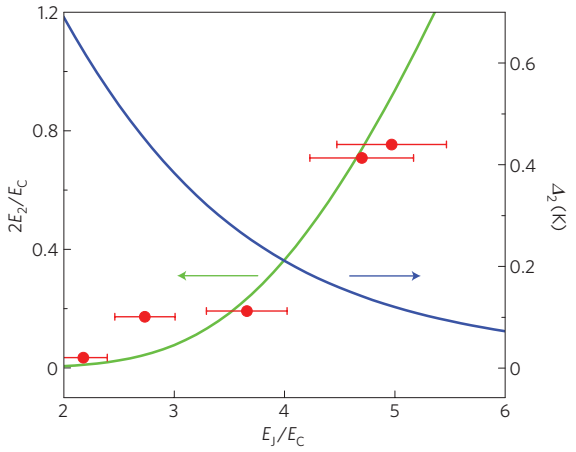

Figure 4 | Characteristic energies $2E_2$ and Δ_2 for the devices with different values of E_J/E_C. The experimental points show the potential barrier $2E_2$ between the states $|0\rangle$ and $|\pi\rangle$ of rhombi arrays calculated from the measured amplitude of the $\Delta\Phi_L = \Phi_0/2$ oscillations of switching current, $I_2 = 4eE_2/\hbar$ (the parameters of individual Josephson junctions in the studied devices are listed in Table 1). The horizontal error bars correspond to the uncertainty in E_J/E_C estimated from the scattering of areas of individual Josephson junctions. The dependencies of $2E_2/E_C$ and Δ_2 on E_J/E_C (green and blue curves, respectively) show the results of numerical calculations for a 4×3 rhombi array (for details, see Supplementary Information). Note that no fitting parameters are involved in the comparison between the calculations and experimental data.

too-large values of E_J/E_C and, thus, numerical simulations (see Supplementary Information). Figure 4 shows that large values of both E_2 and Δ_2 required for protection can be realized for the studied qubit design within the range $E_J/E_C \sim 3$–5.

Another probe of quantum fluctuations in the studied array is provided by the measurements of the effect of the gate voltage on the switching current. In the absence of quantum fluctuations, the critical current of the device coincides with the critical current of three rhombi chains connecting the central strip to one of the leads. Quantum fluctuations, which result in tunnelling of the phase of the central strip between 0 and π, reduce I_{SW}. The offset charge $\Delta q = V_g/C_g$ induced by the gate modulates the phase of the tunnelling amplitudes $t_{isl} \rightarrow t_{isl}\exp(i\Delta q\Delta\phi)$, affecting the interference of processes with $\Delta\varphi = \pm\pi$. Thus, in the presence of quantum fluctuations, we might expect to observe modulation of I_{SW} by V_g. Indeed, Fig. 5a,b shows that for the device with $E_J/E_C = 4.7$, the switching probability oscillates with the gate voltage V_g. The amplitude of oscillations, ΔI_{SW}, in the protected regime $\Phi_R \approx \Phi_0/2$ is in good agreement with our calculations of the dependence $\Delta I_2(E_J/E_C)$ (note that no fitting parameters are involved in this comparison). The period of oscillations, which corresponds to charging of the central 'island' with charge $2e$, is approximately the same for both $\Phi_R = 0$ (Fig. 5a) and $\Phi_R = \Phi_0/2$ (Fig. 5b). This is expected for relatively long (1 ms) current pulses used in these measurements: although the transport of single Cooper pairs is suppressed by quantum fluctuations in this regime, there is still a considerable probability of tunnelling of a Cooper pair to/from the island over a long timescale.

Discussion and summary

The reported data suggest that the topological protection can be realized in a Josephson circuit with a properly tuned ratio E_J/E_C. Our results indicate that (1) the scattering of Josephson junction parameters and individual rhombi areas can be made sufficiently small for the realization of symmetry-protected superconducting qubits, and (2) our theoretical model captures all of the essential features of real devices. Further reduction of the Josephson junction dimensions (larger E_C), with a simultaneous increase of the transparency of the tunnel barrier (larger E_J), will enable an increase of the operational temperature of protected qubits.

Vanishing of the I_{SW} oscillations with the period $\Delta\Phi_L = \Phi_0$ in the protected regime suggests that the supercurrent of single Cooper pairs, $I_1 \equiv 2eE_1/\hbar$, is blocked by quantum fluctuations. In other words, single Cooper pairs become localized in the array when the effective Josephson energy of a rhombus, $V_R = E_{2R}\cos(2\pi\Phi_R/\Phi_0)$, becomes small. Note that in the charge basis, two states of a logical qubit differ by the parity of the number of Cooper pairs. Observation of the oscillations with the period $\Delta\Phi_L = \Phi_0/2$ in the protected regime indicates that the supercurrent is carried by correlated pairs of Cooper pairs with charge $4e$ (refs 18–20). To the best of our knowledge, this is the first observation of the coherent transport of pairs of Cooper pairs in a small-size rhombi array in the quantum regime. The persistence of this phenomenon in larger arrays would imply the appearance of a new thermodynamic phase characterized by $\langle\cos 2\varphi\rangle \neq 0$ in the absence of conventional Cooper pair coherence. This phase can be regarded as 'superconductor nematic'; the global state of the whole array in this phase is characterized by the Z_2 topological order parameter (which takes values either $+1$ or -1) (refs 18–20).

The rhombi array studied here can be used as a qubit protected in its 'idle' state from all local noises in the fourth order if one of the leads is replaced with an island disconnected from the outside world. To carry out a generic gate operation, the qubit

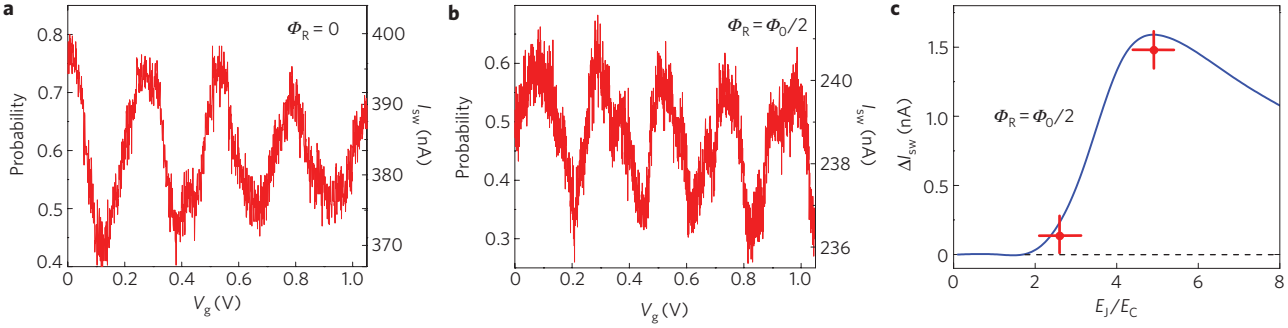

Figure 5 | Gate voltage dependence of the switching current. a,**b**, The probability of switching into the resistive state as a function of the gate voltage for the device with $E_J/E_C \sim 4.7$, measured with a fixed amplitude of current pulses. This probability can be directly translated into the value of the switching current shown on the right vertical axes. **c**, The amplitude of modulation of the switching current, ΔI_{SW}, measured for two devices with different values of E_J/E_C in the regime $\Phi_R = \Phi/2$. The vertical error bars reflect the uncertainty in I_{SW} measurements; the horizontal error bars correspond to the uncertainty in E_J/E_C estimated from the scattering of areas of individual Josephson junctions. The experimental data are in good agreement with the result of the numerical calculation (the blue curve); no fitting parameters are involved in this comparison.

protection has to be temporarily removed. This will result in a faster decoherence, which is equivalent to a loss of the operation precision. Note, however, that the time required for a single operation ($\tau_0 \sim \hbar/\Delta_2 \sim 1$ ns) is expected to be about three orders of magnitude shorter then the decoherence time of the unprotected qubit. In addition, only a small fraction of qubits are addressed at a given moment of time, whereas all other qubits involved in computation remain in the protected state. This strongly decreases the effective error rate of the whole logical qubit. Thus, the possibility to 'turn off' decoherence in the idle state markedly reduces the redundancy required for the implementation of error correction schemes[1,2].

Moreover, the present qubit design enables a large (although incomplete) set of operations in the protected state. The idea of these operations (for a different protected qubit design) was discussed in ref. 27. The essential ingredient of this scheme is a variable coupling of a protected qubit to a large inductor $L \gg (\hbar/2e)^2 E_J^{-1}$. Such a coupling can be provided by a chain of SQUIDs (ref. 28). In the idle state of the qubit, each SQUID is frustrated by the magnetic flux $\Phi_0/2$, which results in zero coupling. The current pulse in the control line shifts the flux in SQUIDs away from its 'idle' value ($\Phi_0/2$) and couples the qubit to the inductor for a short time $\sim\tau_0$. The effect of this coupling is equivalent to the fault-tolerant $R(\pi/4) = \exp(i\pi/4\sigma^z)$ unitary operation[29]. The two-qubit gates can be implemented similarly. Together with the measurements and $R(\pi/8)$ rotations, these operations are sufficient for an arbitrary quantum computation[29,30]. Although $R(\pi/8)$ rotation cannot be implemented in a fault-tolerant manner, the error rates acceptable for this operation are remarkably large ($\sim$0.5) provided that all other operations are fault tolerant (ref. 30). We conclude that the protected qubit design discussed here might provide us with an almost fault-tolerant scheme of quantum computation.

Methods

The Coulomb energy of individual Josephson junctions in rhombi, E_C, should be at least 0.5–1 K to satisfy the requirement $k_B T \ll \Delta_2 < 0.5E_C$ in our experiments conducted at $T \sim 30$–50 mK. Taking into account that the specific capacitance of Al_2O_3-based tunnel barriers is $\sim$50 fF μm^{-2} (ref. 31), the latter condition translates into submicrometre in-plane dimensions of individual Josephson junctions. The devices were fabricated using multi-angle electron-gun deposition of Al films through a nanoscale lift-off mask. Josephson junctions were formed between the aluminium strips of a well-controlled width overlapping at the right angle. To suppress quantum fluctuations in two large (0.3×0.3 μm^2) Josephson junctions, they were shunted by an inter-digitized capacitor $C_{ID} \sim 3 \times 10^{-14}$ F.

For protection from external high-frequency noise and non-equilibrium quasiparticles, the device was flanked by two meander-type inductances L. The thickness of the horizontal Al strips in the meanders shown in Fig. 2d is a factor of 2–3 smaller than that in the vertical strips. Because of the superconducting gap variations within each meander's segment (the critical temperature in Al films substantially depends on their thickness in the range of $\sim$10–30 nm), the meanders 'trap' non-equilibrium quasiparticles generated outside the device[32,33]. The charging effects in the device were probed by applying the gate voltage V_g to the gate capacitor $C_g \sim 2 \times 10^{-18}$ F connected to the central 'island' common to all chains.

Received 2 January 2008; accepted 27 October 2008; published online 30 November 2008

References

1. Steane, A. M. Overhead and noise threshold of fault-tolerant quantum error correction. *Phys. Rev. A* **68**, 042322 (2003).
2. Knill, E. Quantum computing with realistically noisy devices. *Nature* **434**, 39–44 (2005).
3. Steffen, M. *et al.* Measurements of the entanglement of two superconducting qubits via state tomography. *Science* **313**, 1423–1425 (2006).
4. Yoshihara, F. *et al.* Decoherence of flux qubits due to 1/f flux noise. *Phys. Rev. Lett.* **97**, 167001 (2006).
5. Schreier, J. A. *et al.* Suppressing charge noise decoherence in superconducting charge qubits. *Phys. Rev. B* **77**, 180502(R) (2008).
6. Ithier, G. *et al.* Decoherence in a superconducting quantum bit circuit. *Phys. Rev. B* **72**, 134519 (2005).
7. Faoro, L. & Ioffe, L. B. Quantum two level systems and Kondo-like traps as possible sources of decoherence in superconducting qubits. *Phys. Rev. Lett.* **96**, 047001 (2006).
8. Faoro, L. & Ioffe, L. B. Microscopic origin of critical current fluctuations in large, small, and ultra-small area Josephson junctions. *Phys. Rev. B* **75**, 132505 (2007).
9. Aharonov, D., Kitaev, A. & Preskill, J. Fault-tolerant quantum computing with long-range correlated noise. *Phys. Rev. Lett.* **96**, 050504 (2006).
10. Aliferis, P., Gottesman, D. & Preskill, J. Quantum accuracy threshold for concatenated distance-3 codes. *Quantum Inform. Comput.* **6**, 97–165 (2006).
11. Oh, S. *et al.* Elimination of two level fluctuators in superconducting quantum bits by an epitaxial tunnel barrier. *Phys. Rev. B* **74**, 100502(R) (2006).
12. Martinis, J. M. *et al.* Decoherence in Josephson qubits from dielectric loss. *Phys. Rev. Lett.* **95**, 210503 (2005).
13. Vion, D. *et al.* Manipulating the quantum state of an electrical circuit. *Science* **296**, 886–889 (2002).
14. Chioresku, I., Nakamura, Y., Harmans, C. J. P. M. & Mooij, J. E. Coherent quantum dynamics of a superconducting flux qubit. *Science* **299**, 1869–1871 (2003).
15. Pashkin, Yu. A. *et al.* Quantum oscillations in two coupled charge qubits. *Nature* **421**, 823–826 (2003).
16. Wallraff, A. *et al.* Strong coupling of a single photon to a superconducting qubit using circuit quantum electrodynamics. *Nature* **431**, 162–167 (2004).
17. Kitaev, A.Yu. Fault-tolerant quantum computation by anyons. *Ann. Phys.* **303**, 2–30 (2003).
18. Ioffe, L. B. & Feigelman, M. V. Possible realization of an ideal quantum computer in Josephson junction array. *Phys. Rev. B* **66**, 224503 (2002).
19. Doucot, B., Feigelman, M. V. & Ioffe, L. B. Topological order in the insulating Josephson junction arrays. *Phys. Rev. Lett.* **90**, 107003 (2003).
20. Doucot, B., Feigelman, M. V., Ioffe, L. B. & Ioselevich, A. S. Protected qubits and Chern-Simons theories in Josephson junction arrays. *Phys. Rev. B* **71**, 024505 (2005).
21. Blatter, G., Geshkenbein, V. B. & Ioffe, L. B. Design aspects of superconducting-phase quantum bits. *Phys. Rev. B* **63**, 174511 (2001).
22. Doucot, B. & Vidal, J. Pairing of cooper pairs in a fully frustrated Josephson-junction chain. *Phys. Rev. Lett.* **88**, 227005 (2002).
23. Protopopov, I. V. & Feigelman, M. V. Anomalous periodicity of supercurrent in long frustrated Josephson-junction rhombi chains. *Phys. Rev. B* **70**, 184519 (2004).
24. Tinkham, M. *Introduction to Superconductivity* 2nd edn (Dover, 1996).
25. Doucot, B. & Ioffe, L. B. Voltage–current curves for small Josephson junction arrays: Semiclassical treatment. *Phys. Rev. B* **76**, 214507 (2007).
26. Pop, I. M. *et al.* Measurement of the current-phase relation in Josephson junction rhombi chains. *Phys. Rev. B* **78**, 104504 (2008).
27. Kitaev, A. Protected qubit based on a superconducting current mirror. Preprint at <http://arxiv.org/abs/cond-mat/0609441> (2006).
28. Corlevi, S., Guichard, W., Hekking, F. & Haviland, D. B. Phase-charge duality of a Josephson junction in a fluctuating electromagnetic environment. *Phys. Rev. Lett.* **97**, 096802 (2006).
29. Gottesman, D., Kitaev, A. & Preskill, J. Encoding a qubit in an oscillator. *Phys. Rev. A* **64**, 012310 (2001).
30. Bravyi, S. & Kitaev, A. Universal quantum computation with ideal Clifford gates and noisy ancillas. *Phys. Rev. A* **71**, 022316 (2005).
31. Lichtenberger, A. W. *et al.* Fabrication of Nb/Al–Al_2O_3/Nb junctions with extremely low leakage currents. *IEEE Trans. Magn.* **25**, 1247–1250 (1989).
32. Lutchyn, R. M., Glazman, L. I. & Larkin, A. I. Kinetics of the superconducting charge qubit in the presence of a quasiparticle. *Phys. Rev. B* **74**, 064515 (2006).
33. Aumentado, J., Keller, M. W., Martinis, J. M. & Devoret, M. H. Nonequilibrium quasiparticles and 2e periodicity in single-Cooper-pair transistors. *Phys. Rev. Lett.* **92**, 066802 (2004).

Acknowledgements

We thank J. Sanchez and S. Pereverzev for help with experiments and O. Buisson, W. Guichard, L. Faoro, M. Feigelman, B. Pannetier and V. Schmidt for stimulating discussions. The work at Rutgers University was supported in part by the NSF grant ECS-0608842 and the Rutgers Academic Excellence Fund. The work at the University of Paris has been partly supported by the ANR grant ANR-06BLAN-0218-01.

Additional information

Supplementary Information accompanies this paper on www.nature.com/naturephysics. Reprints and permissions information is available online at http://npg.nature.com/reprintsandpermissions. Correspondence and requests for materials should be addressed to M.E.G.